Intraneuronal immunoreactivity for the prion protein distinguishes a subset of E200K genetic from sporadic Creutzfeldt-Jakob Disease

Kovacs, Gabor G ; Molnár, Kinga ; Keller, Eva ; Botond, Gergő ; Budka, Herbert ; László, Lajos

Abstract: Recently, we reported widespread intraneuronal prion protein (PrP) immunoreactivity in genetic Creutzfeldt-Jakob disease (CJD) associated with the E200K mutation. Here, we evaluated 6 cases ofsporadic CJD MM type 1, 5 MV type 2, and 7 VV type 2 and compared their anatomical appearance with that of 29 E200K genetic CJD (gCJD) cases. We also performed double immunolabeling for ubiquitin, p62, early endosomal marker rab5, and immunogold electronmicroscopy in 3 cases. We identified 4 morphological types of intraneuronal PrP immunoreactivity: one type, defined as multiple globular structures, was significantly associated with a subset of E200K gCJD cases and was distinct from the intraneuronal small dotlike PrP immunoreactivity seen in sporadic CJD. Whereas the latter colocalized with rab5, there were single large (7.5 m-15 m) globular inclusion body-like structures detected predominantly but not exclusively in E200K gCJD; these were immunoreactive in part for ubiquitin and p62 and showed focal -tubulin immunoreactivity, suggesting aggresome features. Ultrastructural examination using immunogold revealed PrP localization in aggresome-like structures and in autophagic vacuoles. These findings suggest that the permanent production of mutant PrP in the E200K gCJD cases overwhelms the ubiquitin-proteasome system and shifts the balance toward selectivemacroautophagy and/or to ubiquitinated inclusion body and aggresome formation as a cytoprotective effort to sequester the mutant protein.

DOI: https://doi.org/10.1097/NEN.0b013e318248aa70

Intraneuronal immunoreactivity for the prion protein distinguishes E200K genetic from sporadic Creutzfeldt-Jakob disease

Gabor G. Kovacs MD PhD[1,2], Kinga Molnár PhD[3], Eva Keller MD PhD[4], Gergő Botond[1,3], Herbert Budka MD MScDhc[1], Lajos László PhD[3]

[1]Institute of Neurology and Austrian Reference Center for Human Prion Diseases, Medical University of Vienna, Vienna, Austria
2: Semmelweis University, Neuropathology and Prion Disease Reference Center, Budapest, Hungary
[3]Department of Anatomy, Cell and Developmental Biology, Eötvös Lóránd University of Sciences, Budapest, Hungary;
4: Semmelweis University Department of Forensic Medicine and Insurance Medicine, Budapest, Hungary

Word count title: 9
Word count abstract: 195
Word count text: 3047
Number of Figures: 4
Number of references 49

Running head title: Intraneuronal PrP in E200K genetic CJD

Correspondence to:
Lajos László PhD, Department of Anatomy, Cell- and Developmental Biology, Eötvös Loránd University of Sciences, Budapest, Hungary.
Tel/Fax: +36 1 372 2700/8641; Email: laszlo@elte.hu

Abstract

Recently we reported widespread intraneuronal PrP immunoreactivity in genetic Creutzfeldt-Jakob disease (CJD) associated with the E200K mutation. Here we evaluated six cases of sporadic CJD MM type 1, five MV type 2, and seven VV type 2 and compared the anatomical appearance with 29 E200K genetic CJD cases. In addition, we performed double immunolabeling for ubiquitin, p62, early endosomal marker rab5, and immunogold electron microscopy in three cases. Four morphological types of intraneuronal PrP immunoreactivity were distinguished: one type defined as multiple globular structures was significantly associated with a subset of E200K gCJD cases and was distinct from the intraneuronal small dot-like PrP immunoreactivity seen in sporadic CJD. While the latter colocalized with rab5, single large (7.5-15 μm) globular inclusion body-like structures were detected predominantly but not exclusively in E200K gCJD, immunostained in part for ubiquitin and p62, and showed focal γ-tubulin immunoreactivity, suggesting the character of aggresomes. Indeed, ultrastructural examination revealed PrP localization in aggresome-like structures and in autophagic vacuoles. This suggests that the permanent production of mutant PrP overwhelms the ubiquitin-proteasome system and shifts the balance towards selective macroautophagy and/or to ubiquitinated inclusion-body and aggresome formation, as a cytoprotective effort to sequester the mutant protein.

Key words: prion protein, aggresome, autophagy, endosome-lysosome, ubiquitin-proteosome, p62

Introduction

Prion diseases belong to the group of neurodegenerative disorders and are characterised by deposition of the disease-associated conformer of the cellular prion protein (PrP^{C}), termed PrP^{Sc} in the brain (1). Neurodegenerative diseases are classified according to the predominant protein that accumulates extracellularly as plaques, in synapses, or intracellularly as inclusion bodies (2). The protein-based classification of conformational neurodegenerative diseases underpins the importance of cellular systems involved in protein housekeeping. PrP, as an aggregate-prone protein, is expected to stimulate the clearance mechanisms of the affected cells. The main components of this housekeeping protein degradation network are the ubiquitin proteasome system (UPS) and the autophagy-lysosome pathway (ALP) (3). In addition, large intracellular protein inclusions called aggresomes have been described as key organelles in the segregation and clearance of toxic cytoplasmic misfolded proteins (4, 5).

Although our knowledge on the intracellular trafficking and the fate of PrP is incomplete, there are already remarkable observations to support the role of these pathways (6, 7). Similarly to amyloid-beta (Aβ) in Alzheimer`s disease (AD), the processing of PrP and the conversion of PrP^{C} into PrP^{Sc} most likely involves the endosome-lysosome system (ELS) (8-13). Intraneuronal PrP immunoreactivity (IR) has been described in idiopathic or sporadic Creutzfeldt-Jakob disease (CJD), in particular associated with type 2 proteinase resistant PrP (14, 15), as well as in different animals and experimental models (16-19). These must be distinguished from diffuse neuronal PrP immunostaining detected also in non-diseased individuals, most likely representing the cellular form of PrP (20). Hovewer, in contrast to tau, alpha-synuclein, TDP-43 (TAR-DNA binding protein), and FUS (fused in sarcoma protein), PrP^{Sc} has not yet been reported to regularly form intracellular inclusions, defined as ubiquitinated aggregates, but deposits preferably in synapses or accumulates in the form of plaques extracellularly (1). It must be noted, however, that a study on ubiquitin immunostaining in CJD reported that cortical nerve cells contained scanty ubiquitinated dot-like inclusions (21), furthermore, inclusion-body like PrP immunopositivity was also reported in sporadic CJD (22, 23). The *in vitro* findings in prion infected cells that the inhibition of proteasomes lead to aggresome formation raises the possibility that aggresomes participate in the sequestration of PrP^{Sc} (24, 25). Nevertheless, aggresomes have not yet been documented in human prion disease, thus this potentially cytoprotective mechanism seem to have less relevance for the pathogenesis of human disease.

One of the most frequent mutations associated with genetic prion disease of the CJD phenotype is

associated with the E200K mutation in the prion protein gene (*PRNP*). Recently, a systematic study on E200K genetic CJD demonstrated intracellular deposition of disease-associated PrP as a frequent event (26); there we reported it in approximately 33% of codon 129 MM homozygote cases and in 71% of MV heterozygotes. We also demonstrated (see supplemental material of Ref. 26) that they appear in subcortical regions and brainstem nuclei regularly, and may be prominent in deeper layers of the neocortex and CA1 subregion of the hippocampus. In the present study we further characterize these intracellular PrP deposits and demonstrate that their distribution and morphology distinguishes them from neuron-related PrP IR seen in sporadic CJD cases. Moreover, we find them not only in relation to the ELS, but partly forming aggresome-like structures.

Material and methods

Selection of cases

We examined six cases of sporadic CJD MM type 1 (3 women, 3 men; mean duration of illness in months $\pm$ standard deviation: 3.3 + 0.5; mean age at death in years: 70 $\pm$ 2.8), five MV type 2 (3,2; 19.8 + 16.2; 67.6 $\pm$ 4.2), and seven VV type 2 (1, 6; 9.2 $\pm$ 8.4; 69 $\pm$ 4.8), to evaluate how many cases show neuron-related PrP. In these cases we examined the morphological spectrum of neuronal-related PrP IR and compared the anatomical predominance with 29 E200K genetic CJD (15 MM, 13 MV and 1 VV) cases (26). Post mortem delay varied between 12 and 36 hours. The study was performed within a project ("Molecular neuropathologic investigation of neurodegenerative diseases") approved by the Ethical Committee of the Medical University of Vienna and is in accordance with the Helsinki Declaration of 1975.

Immunohistochemistry

For immunohistochemistry 5 mm thick sections of formalin-fixed and paraffin-embedded tissue were used with primary antibodies listed here: anti-PrP 12F10 (1:1,000, Cayman Chemical, Ann Arbor, MI, USA, epitope: aa. 142-160), anti-PrP BG4 (1:1000, TSE Resource Centre, Birkett CR, Compton, U.K.; epitope: aa. 23-85), monoclonal mouse anti-p62 (1:1000, BD Transduction, Lexington KY, USA), monoclonal mouse anti-ubiquitin (1:50,000, Millipore, Temecula, CA, USA), polyclonal rabbit anti-γ-tubulin (1:500, Santa Cruz. Santa Cruz, CA, USA), polyclonal rabbit anti-rab5 (1:500, Calbiochem, San Diego, CA), anti-tau AT8 (pS202, 1:200, Pierce Biotechnology, Rockford, IL, USA), anti-phospho-TDP-43 (pS409/410, 1:2,000, Cosmo Bio, Tokyo, Japan), anti-α-synuclein (1:10,000, clone 4D6, Signet, Dedham, MA, USA), anti-Aβ (1:50, clone 6F/3D, Dako, Glostrup, Denmark). The DAKO EnVision© detection kit, peroxidase/DAB, rabbit/mouse (Dako, Glostrup, Denmark) was used for visualization of antibody reactions.

Evaluation of intraneuronal PrP immunoreactivities (see below) was performed with a dichotomous approach (yes/no) in the following anatomical regions: frontal, cingular, parietal, temporal, occipital cortex upper and deeper layers; caudate nucleus, putamen, globus pallidus, thalamus medial and lateral nuclei; hippocampus CA1 subregion and subiculum; raphe nuclei, pontine base nuclei, inferior olives, and dentate nucleus.

Double immunolabeling was performed using monoclonal anti-PrP (12F10), and anti-ubiquitin and polyclonal anti-rab5. The fluorescence-labeled secondary antibodies were Alexa Fluor (AF) 555 donkey anti-mouse IgG (1:200; Molecular Probes, Inc., Eugene, OR, USA), AF 488 goat anti-rabbit (1:200; Molecular Probes, Inc.), Zenon AF 488 Mouse IgG_1 (Molecular Probes, Inc.). The following combinations were applied: PrP/Ubiquitin (including Zenon AF) and PrP/Rab5. Double immunolabeling involving anti-PrP antibody was performed after pretreatment of the section with 20 min heat-induced epitope retrieval with citrate buffer (pH6) followed by 2 min formic acid (96%). We evaluated double immunofluorescent labeling with a Zeiss LSM 510 confocal laser microscope.

Statistical analysis

Chi-square statistics was performed to evaluate the proportion of cases showing different types of intraneuronal PrP IR and the proportion of involved anatomical regions showing intraneuronal PrP IR in those cases, which showed this type of IR. P value below 0.05 was considered significant.

Paraffin-embedded tissue (PET) blotting

This was performed with slight modifications according to published protocols (27). Briefly, sections of formalin fixed, paraffin embedded brain tissue (the same anatomical region as used for immunohistochemistry and electron microscopy) was placed onto a nitrocellulose membrane. Sections were treated with Proteinase K (Sigma-Aldrich) for eight hours in 56°C. After washing, we treated the membranes with 3 M Guanidin Isothiocyanate for 10 minutes. For immunodetection we used antibody 3F4 (1:500, monoclonal mouse, Signet).

Immunoelectron microscopy

After incubation of the deparaffinised tissue sections with anti-PrP (12F10) antibody, we applied ultrasmall gold conjugated secondary antibody (Aurion, Wageningen, The Netherlands) followed by silver-enhancing method. Slides were mounted with resin and examined in light microscopy. Selected areas containing immunoreactive cells were re-embedded for ultrathin sectioning (28). We used a JEOL-1011 electron microscope to analyse the ultrastructural localization of PrP-specific

immunolabeling in the ultrathin sections.

Results

Morphological spectrum of intraneuronal PrP IR

We distinguished the following types of neuronal PrP immunopositivities (Fig. 1A):

Type I: Diffuse cytoplasmic PrP IR without distinct granular or dot-like appearance. We have evaluated this type in a previous comprehensive study (20).

Type II: Many tiny dots in the perikaryon. Sometimes these exhibit a granular appearance of IR. The size of the dots ranges between 0.2 and 1.0 μm.

Type III: Distinct small globular darkly immunostained cytoplasmic PrP immunopositive profiles. These are always multiple but their number is less than of type II (usually 5-10), and their size is larger, ranging between 1.5 and 4.0 μm.

Type IV: Distinct single larger globular structures with a size similar to that of the nuclei of the neuron, with a range between 7.5 and 15 μm.

In addition, prominent diffuse/synaptic PrP IR is associated with the so called "somato-synaptic" pattern defined as tiny dots scattered in or above the microscopic focus-level of the neuronal cytoplasm: this was not considered here and was seen in all subtypes of prion disease involved in our study.

Distribution of intraneuronal PrP IR

When pooling all subtypes of sCJD, there was no significant difference between these regarding the presence of any type of intraneuronal PrP IR.

Type II neuron-related PrP IR was seen mainly in sCJD VV type 2 and also in MV type 2 cases, but not in MM type 1 and less in E200K cases (Fig 1B and Fig 2). When present it appeared in several anatomical regions (Fig 1 C): the proportion of involved regions was significantly higher for gCJD E200K subtypes when compared to subtypes of sCJD except for more regions in sCJD VV type 2 when compared to gCJD E200K MM.

Type III was significantly associated with a subset of E200K gCJD cases (MM, MV, VV) in an anatomical distribution (Figs. 1B, C and 2) that included predominantly the brainstem, thalamus and deeper layers of the cortex (16). Interestingly, where it was available in the examined section, we observed this type in the cells of the periventricular germinal matrix (Fig. 2).

Type IV was predominantly seen E200K cases, however three sCJD VV type 2 (all in lateral thalamus and one in the dentate nucleus as well) and a single MM-1 (dorsal raphe nucleus) also showed similar structures (Figs. 1 C and 2). However, in E200K these were always seen in many neurons, while in sCJD it was observed in single neurons. In addition, in sCJD brains this was not associated with ubiquitin or p62 IR in the same cells.

Light microscopic characterization of intraneuronal PrP IR in E200K gCJD

PET blot for protease-resistant PrP proved that the intracellular immunopositivities are resistant to protease, thus represent disease-associated PrP (Fig. 3 A). Intracellular PrP deposits were not detected with an antibody raised against the N-terminal of PrP (Fig. 3 B). Moreover some cells contained p62 (Fig. 3 C) but more cells showed ubiquitin-immunopositive structures (Fig. 3 D, E) that were immunonegative for α-synuclein, phospho-tau (AT8), phospho-TDP-43, and FUS. In addition, occasional neurons with type IV intraneuronal PrP IR exhibited perinuclear γ-tubulin IR structures (Fig. 3 F). Double immunolabeling for ubiquitin and disease-associated PrP confirmed that these inclusion-body-like structures are partly ubiquitinated (Fig. 3 G), while the smaller dot-like PrP IR (type II and III) partly co-localized with the early endosomal marker, rab5 (Fig. 3 H).

Ultrastructural observations

We observed several large PrP-positive intracellular protein inclusions about the size of the nucleus in the neurons of the inferior olive (Fig. 4 A, B). Immunogold particles representing disease-associated PrP accumulated within huge aggresome-like structures in the neighbourhood of the nucleus (Fig. 4 A, B). Further PrP-positive granules (Fig. 4 C) were seen in the close vicinity of the rough endoplasmic reticulum (RER). The compact appearance of these particles strongly resembled pre-aggresomes (Fig. 4 D). Some neurons contained PrP-positive aggregates sequestered in spherical, membrane-bound autolysosome-like organelles (Fig. 4 E). Several small vesicles and multivesicular bodies also showed PrP-specific immunolabeling (Fig. 4 F, G).

Discussion

Here we document neuronal intracytoplasmic inclusion body formation composed of the disease-associated PrP in genetic CJD associated with the E200K mutation in the *PRNP*. We could compare light microscopy with the ultrastructural immunodetection of the disease-associated PrP in exactly the same selected neurons in human tissue (28). In spite of the limitations of *post mortem* paraffin-embedded tissue for electron microscopical evaluation, our *in vivo* results support *in vitro* studies addressing the issue of how the disease-associated (mutant) PrP is processed in the cytoplasm and whether it may form intracellular aggregates.

Punctuate intraneuronal PrP immunoreactivity was observed in animals and experimental models of prion disease as well as in sporadic CJD, usually associated with certain molecular subtypes (7, 14-19). In addition, inclusion-body-like structures were reported in five out of eight individuals with panencephalopathic type of CJD (without data on the codon 129) in the dentate nucleus (23) and in another report in the thalamus (22). Although, intraneuronal ubiquitin immunoreactivity was also mentioned in a study (21), here we show that indeed large ubiquitinated inclusions may appear in CJD brains. In spite the presence of intraneuronal PrP IR in both sporadic and genetic CJD, our present study indicates that a certain morphological type (type III) is distinctive for the E200K genetic CJD cases. Interestingly, similar prominent intraneuronal PrP IR was described recently in a mouse model of the E200K mutation (29). In addition, the inclusion body-like structures (type IV) always involved more neurons in genetic as in sporadic CJD cases. Anatomically, the dentate, the inferior olivary nucleus, and pontine base neurons showed mostly these. A comprehensive study of intraneuronal PrP in sheep brains, comparing the dorsal motor nucleus of the vagus and the olivary nuclei, already suggested that the variability in PrP processing by neurones could be cell-dependent (19).

Co-localization of the early-endosomal marker Rab5 and the mutant disease-associated PrP, and the presence of PrP in multivesicular bodies support a role for the ELS in the pathogenesis of human genetic prion disease. Several studies have shown the involvement of the ELS in experimental models of prion disease and also in sporadic CJD (8-11, 30). Indeed, it was recently shown that a mild acidic pH is needed for the destabilization of the human codon E200K mutant PrP, underpinning the importance of endosomal processing and complementing our morphological observations (31, 32).

In addition to the relation to the ELS, we detected disease-associated PrP in close vicinity of RER

cisterns as well as large (around the size of the neuronal nucleus) globular PrP-immunopositive structures. The relation of mutant PrP to RER cisterns is well in line with the observation that untranslocated cytosolic PrP accumulates in the cytosol, is ubiquitinated and serves as a substrate for proteasomal degradation (6). Indeed, intracellular inclusion body-like structures showed partial ubiquitin and p62 IR. Only extracellular but not intracellular PrP deposits were visualized using an antibody against the N-terminal fragment of PrP. On one hand, the frequently noted smaller intracytoplasmic immunoreactivities most likely represent truncated PrP, in accordance with its co-localization with the early endosomal marker rab5. On the other hand, due to their partial ubiquitin and p62 immunopositivity, the occasional larger inclusion-like bodies most likely have a cytosolic origin, hence their immunonegativity for N-terminal PrP could also suggest conformational masking of the N-terminal epitope.

In addition, the morphological appearance and the partial ubiquitin and p62 immunoreactivities of the large PrP inclusion bodies suggests the activation of autophagy and/or aggresome formation. Recent observations support the notion that ubiquitin attached to the misfolded protein substrates can be a common marker for either the UPS or the p62-mediated selective autophagy (33, 34). Several data have documented the close relation and coordinated activity of the UPS and autophagy. When the cytosolic accumulation of misfolded proteins (i.e. mutant PrP) is permanent and the UPS (or the machinery required for substrate sorting to UPS) is consequently overwhelmed, autophagy may be induced as a compensatory cytoprotective mechanism (35, 36). Noteworthy, significant neuronal autophagy has been reported in scrapie and CJD infected mouse brain as well as in human CJD samples (37-40). Moreover, induction of autophagy enhanced the lysosomal degradation of endosomally internalised PrP^{Sc} in prion-infected cells (41, 42). Nevertheless, further studies are needed to elucidate the exact role of the ubiquitin- and p62-dependent selective autophagy in the clearance of the cytosolic mutant PrP.

In addition to the above mentioned protein housekeeping systems, aggresome formation has been recognized as a secondary defense mechanism. It sequesters and transforms potentially toxic, misfolded aggregate-prone proteins into relatively inert inclusions for further degradation (4, 5, 43). Thus, until now aggresomes have been reported only in *in vitro* prion models using proteasome and chaperone inhibitors, but never in human prion diseases *in vivo*. It has been shown that the retro- and untranslocated PrP accumulates and forms pre-aggresomes and mature aggresomes in neurons (25, 44-46).

It is generally accepted that gCJD with the E200K is not different from sCJD (mainly MM type 1

cases) (47). However, there are several differences to be noted: 1) presence of a distinct type of intraneuronal PrP IR in all codon 129 variants; 2) presence of a stripe-like pattern of PrP IR in the cerebellar cortex that is associated with less prominent spongiform change in the molecular layer (26, 48); 3) trend for more prominent involvement of the deeper layers irrespective of codon 129 constellation (a feature more characteristic of VV type 2 sCJD); 4) lack of amyloid kuru-type plaques in cases with MV at codon 129 even when associated with type 2 proteinase resistant PrP (as characteristic for sporadic CJD MV type 2); and 5) frequent association with other neurodegeneration-related protein deposits.

Our findings in a genetic prion disease (and not in idiopathic forms) argue for the following possibilities. First, the dynamics of protein processing may differ between genetic and idiopathic CJD. In genetic CJD the protein processing systems are constantly overwhelmed, most likely for a longer period, while in idiopathic CJD a more dramatic course can happen with early neuronal death and bursting of the disease-associated PrP into the extracellular space. Second, *post mortem* examinations usually reflect a terminal stage, when neurons have been already damaged and some, seemingly extracellular, globular protein aggregates may represent formerly intracellular aggregates where the neuronal cell body was lysed, analogously to the extracellular Lewy bodies in Parkinson`s disease. Indeed, we and others showed ubiquitination of larger extracellular PrP deposits in sporadic CJD (21, 49). However, this merits further studies in idiopathic CJD and may help to clarify the role of aggresome formation in human prion diseases. From a neuropathological diagnostic point of view, presence of ubiquitin or p62 immunoreactive intracellular inclusions that are negative for TDP-43, FUS, alpha-synuclein, or phospho-Tau in a neurodegenerative disorder might raise the need for additional screening with anti-PrP immunohistochemistry.

In conclusion, our observations support the concept of a complex intracellular pathogenetic scenario involving the disease-associated mutant PrP. According to our and other studies, the major players are the ELS, the UPS, autophagy, and aggresome formation, which interact in a delicate balance. Involvement of this complex system might differ between etiological forms of prion diseases. Since not all aspects described here in genetic prion disease have been observed in sporadic (idiopathic) forms, patients suffering from genetic vs. idiopathic CJD might require distinct therapeutic approaches.

Acknowledgement: Technical assistance of Gerda Ricken, Irene Leisser, and Marianna Lenkeine is highly acknowledged. This study was supported by the Austrian-Hungarian Action Fundation (N^{o} 82öu8; to L.L., K.M., G.G.K.), by the Hungarian Scientific Research Fund (OTKA-NK78012; to L.L., K.M.) and by the European Social Fund (TAMOP 4.2.1./B-09/1/KMR-2010-0003; to L.L.) and TAMOP 4.2.1./B-03/1/KMR-2010-001.

References

1. Kovacs GG, Budka H. Prion diseases: from protein to cell pathology. Am J Pathol 2008:172;555-65.
2. Kovacs GG, Botond G, Budka H. Protein coding of neurodegenerative dementias: the neuropathological basis of biomarker diagnostics. Acta Neuropathol 2010:119;389-408.
3. Rubinsztein DC. The roles of intracellular protein-degradation pathways in neurodegeneration. Nature 2006:443;780-6.
4. Kopito RR. Aggresomes, inclusion bodies and protein aggregation. Trends Cell Biol 2000:10;524-30.
5. Tanaka M, Kim YM, Lee G, Junn E, Iwatsubo T, Mouradian MM. Aggresomes formed by alpha-synuclein and synphilin-1 are cytoprotective. J Biol Chem 2004:279;4625-31.
6. Chakrabarti O, Ashok A, Hegde RS. Prion protein biosynthesis and its emerging role in neurodegeneration. Trends Biochem Sci 2009:34;287-95.
7. Jeffrey M, McGovern G, Siso S, Gonzalez L. Cellular and sub-cellular pathology of animal prion diseases: relationship between morphological changes, accumulation of abnormal prion protein and clinical disease. Acta Neuropathol 2011:121;113-34.
8. Arnold JE, Tipler C, Laszlo L, Hope J, Landon M, Mayer RJ. The abnormal isoform of the prion protein accumulates in late-endosome-like organelles in scrapie-infected mouse brain. J Pathol 1995:176;403-11.
9. Borchelt DR, Taraboulos A, Prusiner SB. Evidence for synthesis of scrapie prion proteins in the endocytic pathway. J Biol Chem 1992:267;16188-99.
10. Laszlo L, Lowe J, Self T, Kenward N, Landon M, McBride T, Farquhar C, McConnell I, Brown J, Hope J, et al. Lysosomes as key organelles in the pathogenesis of prion encephalopathies. J Pathol 1992:166;333-41.
11. Magalhaes AC, Baron GS, Lee KS, Steele-Mortimer O, Dorward D, Prado MA, Caughey B. Uptake and neuritic transport of scrapie prion protein coincident with infection of neuronal cells. J Neurosci 2005:25;5207-16.
12. Marijanovic Z, Caputo A, Campana V, Zurzolo C. Identification of an intracellular site of prion conversion. PLoS Pathog 2009:5;e1000426.
13. Nixon RA, Yang DS, Lee JH. Neurodegenerative lysosomal disorders: a continuum from development to late age. Autophagy 2008:4;590-9.
14. Kovacs GG, Head MW, Bunn T, Laszlo L, Will RG, Ironside JW. Clinicopathological phenotype of codon 129 valine homozygote sporadic Creutzfeldt-Jakob disease. Neuropathology and applied neurobiology 2000:26;463-72.
15. Wemheuer WM, Benestad SL, Wrede A, Schulze-Sturm U, Wemheuer WE, Hahmann U, Gawinecka J, Schutz E, Zerr I, Brenig B, Bratberg B, Andreoletti O, Schulz-Schaeffer WJ. Similarities between forms of sheep scrapie and Creutzfeldt-Jakob disease are encoded by distinct prion types. The American journal of pathology 2009:175;2566-73.
16. Beekes M, McBride PA, Baldauf E. Cerebral targeting indicates vagal spread of infection in hamsters fed with scrapie. J Gen Virol 1998:79 (Pt 3);601-7.
17. Debeer SO, Baron TG, Bencsik AA. Immunohistochemistry of PrPsc within bovine spongiform encephalopathy brain samples with graded autolysis. J Histochem Cytochem 2001:49;1519-24.
18. Gonzalez L, Martin S, Begara-McGorum I, Hunter N, Houston F, Simmons M, Jeffrey M. Effects of agent strain and host genotype on PrP accumulation in the brain of sheep naturally and experimentally affected with scrapie. J Comp Pathol 2002:126;17-29.
19. Gonzalez L, Martin S, Jeffrey M. Distinct profiles of PrP(d) immunoreactivity in the brain of scrapie- and BSE-infected sheep: implications for differential cell targeting and PrP processing. J Gen Virol 2003:84;1339-50.
20. Kovacs GG, Voigtlander T, Hainfellner JA, Budka H. Distribution of intraneuronal

immunoreactivity for the prion protein in human prion diseases. Acta Neuropathol 2002:104;320-6.
21. Ironside JW, McCardle L, Hayward PA, Bell JE. Ubiquitin immunocytochemistry in human spongiform encephalopathies. Neuropathol Appl Neurobiol 1993:19;134-40.
22. Tanaka S, Ota M, Ohama E. A case of sporadic Creutzfeldt-Jakob disease with both plaque and synaptic-type deposition of prion protein. Neuropathology 2000:20;49-55.
23. Tanaka S, Saito M, Morimatsu M, Ohama E. Immunohistochemical studies of the PrP(CJD) deposition in Creutzfeldt-Jakob disease. Neuropathology 2000:20;124-33.
24. Cohen E, Taraboulos A. Scrapie-like prion protein accumulates in aggresomes of cyclosporin A-treated cells. EMBO J 2003:22;404-17.
25. Kristiansen M, Messenger MJ, Klohn PC, Brandner S, Wadsworth JD, Collinge J, Tabrizi SJ. Disease-related prion protein forms aggresomes in neuronal cells leading to caspase activation and apoptosis. J Biol Chem 2005:280;38851-61.
26. Kovacs GG, Seguin J, Quadrio I, Hoftberger R, Kapas I, Streichenberger N, Biacabe AG, Meyronet D, Sciot R, Vandenberghe R, Majtenyi K, Laszlo L, Strobel T, Budka H, Perret-Liaudet A. Genetic Creutzfeldt-Jakob disease associated with the E200K mutation: characterization of a complex proteinopathy. Acta Neuropathol 2011:121;39-57.
27. Schulz-Schaeffer WJ, Tschoke S, Kranefuss N, Drose W, Hause-Reitner D, Giese A, Groschup MH, Kretzschmar HA. The paraffin-embedded tissue blot detects PrP(Sc) early in the incubation time in prion diseases. Am J Pathol 2000:156;51-6.
28. Matej R, Botond G, Laszlo L, Kopitar-Jerala N, Rusina R, Budka H, Kovacs GG. Increased neuronal Rab5 immunoreactive endosomes do not colocalize with TDP-43 in motor neuron disease. Exp Neurol 2010:225;133-9.
29. Friedman-Levi Y, Meiner Z, Canello T, Frid K, Kovacs GG, Budka H, Avrahami D, Gabizon R. Fatal Prion Disease in a Mouse Model of Genetic E200K Creutzfeldt-Jakob Disease. PLoS Pathog 2011:7;e1002350.
30. Kovacs GG, Gelpi E, Strobel T, Ricken G, Nyengaard JR, Bernheimer H, Budka H. Involvement of the endosomal-lysosomal system correlates with regional pathology in Creutzfeldt-Jakob disease. J Neuropathol Exp Neurol 2007:66;628-36.
31. Campos SR, Machuqueiro M, Baptista AM. Constant-pH molecular dynamics simulations reveal a beta-rich form of the human prion protein. J Phys Chem B 2010:114;12692-700.
32. Hasegawa K, Mohri S, Yokoyama T. Fragment molecular orbital calculations reveal that the E200K mutation markedly alters local structural stability in the human prion protein. Prion 2010:4;38-44.
33. Lamark T, Johansen T. Autophagy: links with the proteasome. Curr Opin Cell Biol 2010:22;192-8.
34. Pankiv S, Clausen TH, Lamark T, Brech A, Bruun JA, Outzen H, Overvatn A, Bjorkoy G, Johansen T. p62/SQSTM1 binds directly to Atg8/LC3 to facilitate degradation of ubiquitinated protein aggregates by autophagy. J Biol Chem 2007:282;24131-45.
35. Lamark T, Kirkin V, Dikic I, Johansen T. NBR1 and p62 as cargo receptors for selective autophagy of ubiquitinated targets. Cell Cycle 2009:8;1986-90.
36. Nedelsky NB, Todd PK, Taylor JP. Autophagy and the ubiquitin-proteasome system: collaborators in neuroprotection. Biochim Biophys Acta 2008:1782;691-9.
37. Boellaard JW, Kao M, Schlote W, Diringer H. Neuronal autophagy in experimental scrapie. Acta Neuropathol 1991:82;225-8.
38. Boellaard JW, Schlote W, Tateishi J. Neuronal autophagy in experimental Creutzfeldt-Jakob's disease. Acta Neuropathol 1989:78;410-8.
39. Liberski PP, Sikorska B, Gibson P, Brown P. Autophagy contributes to widespread neuronal degeneration in hamsters infected with the Echigo-1 strain of Creutzfeldt-Jakob disease and mice infected with the Fujisaki strain of Gerstmann-Straussler-Scheinker (GSS) syndrome. Ultrastruct Pathol 2011:35;31-6.
40. Sikorska B, Liberski PP, Giraud P, Kopp N, Brown P. Autophagy is a part of ultrastructural synaptic pathology in Creutzfeldt-Jakob disease: a brain biopsy study. Int J Biochem Cell Biol

2004:36;2563-73.
41. Aguib Y, Heiseke A, Gilch S, Riemer C, Baier M, Schatzl HM, Ertmer A. Autophagy induction by trehalose counteracts cellular prion infection. Autophagy 2009:5;361-9.
42. Heiseke A, Aguib Y, Riemer C, Baier M, Schatzl HM. Lithium induces clearance of protease resistant prion protein in prion-infected cells by induction of autophagy. J Neurochem 2009:109;25-34.
43. Olzmann JA, Li L, Chin LS. Aggresome formation and neurodegenerative diseases: therapeutic implications. Curr Med Chem 2008:15;47-60.
44. Ben-Gedalya T, Lyakhovetsky R, Yedidia Y, Bejerano-Sagie M, Kogan NM, Karpuj MV, Kaganovich D, Cohen E. Cyclosporin-A-induced prion protein aggresomes are dynamic quality-control cellular compartments. J Cell Sci 2011:124;1891-902.
45. Chakrabarti O, Rane NS, Hegde RS. Cytosolic aggregates perturb the degradation of nontranslocated secretory and membrane proteins. Mol Biol Cell 2011:22;1625-37.
46. Mishra RS, Bose S, Gu Y, Li R, Singh N. Aggresome formation by mutant prion proteins: the unfolding role of proteasomes in familial prion disorders. J Alzheimers Dis 2003:5;15-23.
47. Capellari S, Strammiello R, Saverioni D, Kretzschmar H, Parchi P. Genetic Creutzfeldt-Jakob disease and fatal familial insomnia: insights into phenotypic variability and disease pathogenesis. Acta Neuropathol 2011:121;21-37.
48. Jarius C, Kovacs GG, Belay G, Hainfellner JA, Mitrova E, Budka H. Distinctive cerebellar immunoreactivity for the prion protein in familial (E200K) Creutzfeldt-Jakob disease. Acta Neuropathol 2003:105;449-54.
49. Kovacs GG, Preusser M, Strohschneider M, Budka H. Subcellular localization of disease-associated prion protein in the human brain. Am J Pathol 2005:166;287-94.

Figure legends

Figure 1. Types and distribution of intraneuronal PrP immunoreactivities.
A: Different types of intraneuronal PrP immunoreactivities.
B: Distribution of intraneuronal PrP immunoreactivites in sporadic CJD and genetic CJD with E200K mutation.
C: Proportional (%) involvement of examined regions (12 in each case) in cases showing intraneuronal PrP immunoreactivity.

Figure 2. Representative images of intraneuronal immunoreactivities in sporadic (MM type 1: A-C; VV type 2: D-F; MV type 2: G-I) and genetic CJD (E200K: MV: J, K, L, N; VV: O; MM: M) in the following anatomical regions: Dentate nucleus: F, I; Inferior olive: E, H, L; Hippocampus (CA4): D; Thalamus: A, G, K; Pons base: B, N, O; Caudate nucleus: C; Colliculus inferior: J; Germinal matrix: M. Scale bar in A represents 10 μm in A-C, E, H, I, M, 20 μm for D, J-L, and 7.5 μm for M-O.

Figure 3. Light microscopic detection of disease associated PrP.
A: PET blot for protease-resistant PrP (hippocampus CA1; representative gCJD E00K MV case). B: Intracellular PrP deposits are not detected with an antibody raised against the N-terminal of PrP (left, frontal cortex; representative gCJD E00K MV case) that otherwise strongly labels extracellular PrP (right). Immunostaining for p62 (C, frontal cortex; representative gCJD E00K MV case) and ubiquitin (D, E, frontal cortex: D and E left, inferior olive: E right; representative gCJD E00K MV case) demonstrates intracellular immunopositive structures. F: Immunostaining for PrP (left) and γ-tubulin (right, adjacent sections, pontine nuclei neuron from gCJD E200K VV case). Double immunolabeling for ubiquitin and disease-associated PrP confirms that these inclusion body-like structures are partly ubiquitinated (G,), while the smaller dots-like PrP IR partly co-localizes with the early endosomal marker, rab5 (H) (both frontal cortex, representative gCJD E00K MV case). Scale bar in A represents 10 μm in A, C, E, F, G, H and 25 μm for B and D.

Figure 4. Ultrastructural localization of disease associated PrP.
A and C: Electron micrographs demonstrate inferior olive neurons containing large PrP-immunoreactive cytoplasmic inclusions. In the light microscopic insets, the arrows indicate the cells that are selected for ultrastructural investigation. A significant accumulation of electron-dense silver particles corresponding to disease-associated PrP (arrowheads) can be observed in an aggresome-like structure of about the size of the nucleus (B), in the close-vicinity of RER (D) and in spherical

autolysosome-like vacuoles (E). Panel G, as a magnified part of panel F, shows a multivesicular body containing PrP-specific labeling (arrow) in a lipofuscin (L) rich neuron. Scale bars represent 2 μm in panel A, C and F, and 0.4 μm in panel B, D and G.

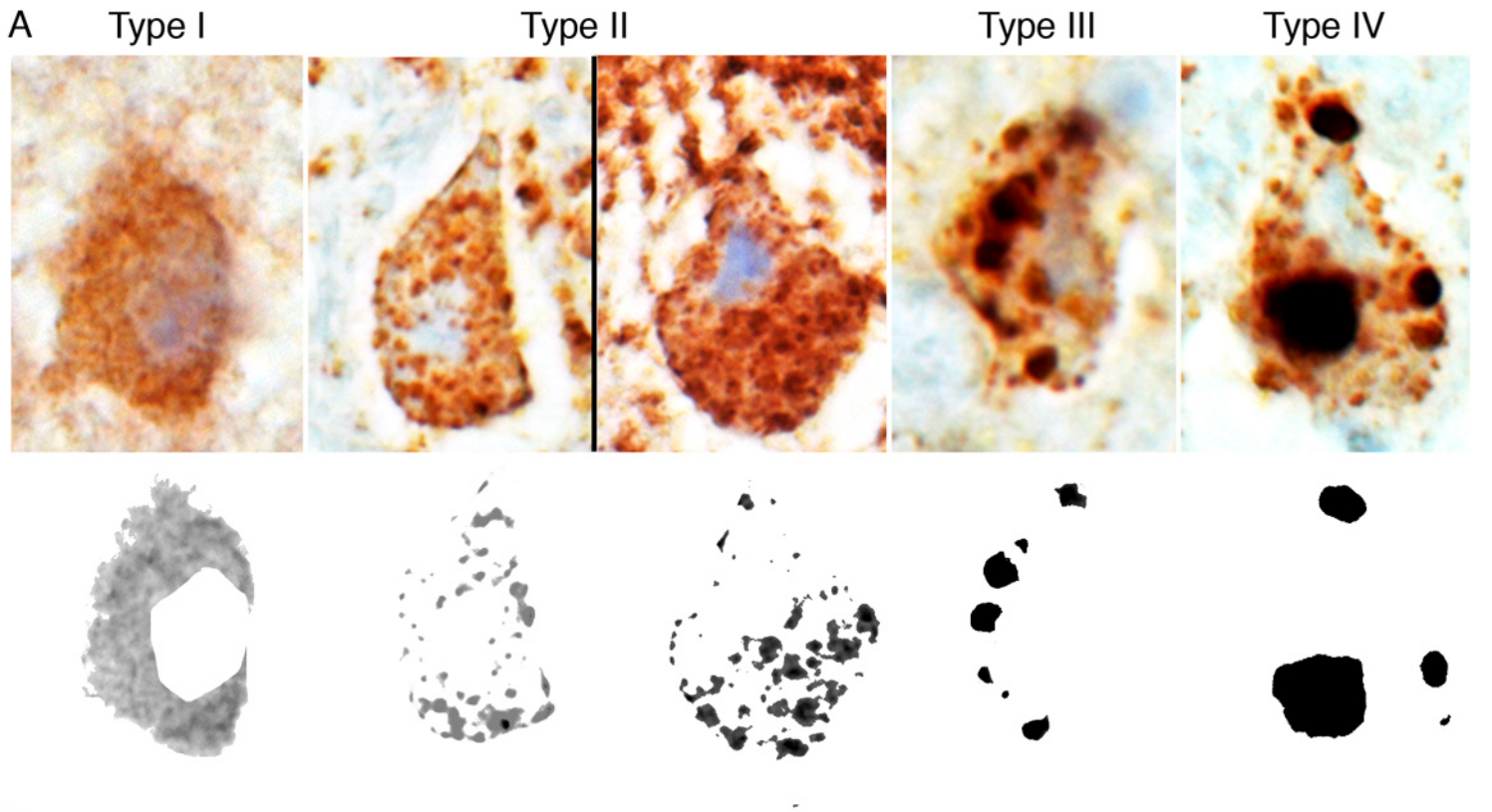
A
Type I
Type II
Type III
Type IV

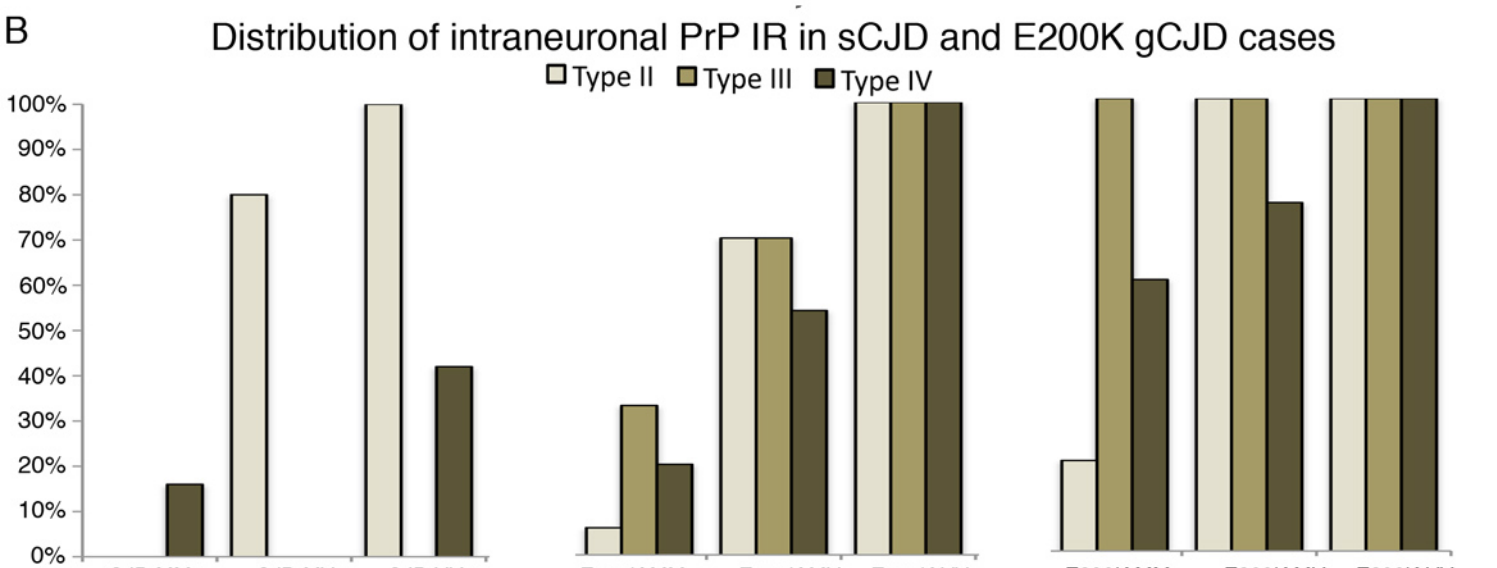
B
Distribution of intraneuronal PrP IR in sCJD and E200K gCJD cases
Type II
Type III
Type IV
100%
90%
80%
70%
60%
50%
40%
30%
20%
10%
0%
sCJD MM1
sCJD MV2
sCJD VV2
E200K MM
E200K MV
E200K VV
All examined cases
Cases with INIR (type III)
n= 6 5 7
n= 15 13 1
n= 5 9 1

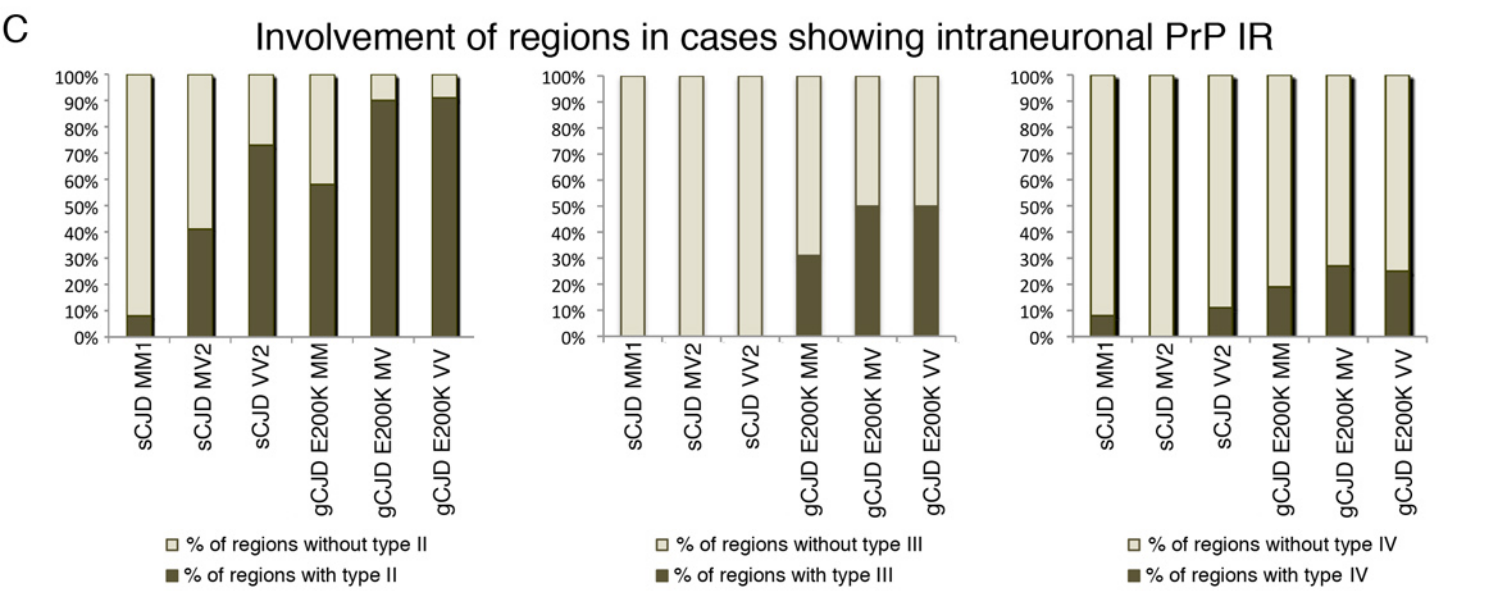
C
Involvement of regions in cases showing intraneuronal PrP IR
100%
90%
80%
70%
60%
50%
40%
30%
20%
10%
0%
sCJD MM1
sCJD MV2
sCJD VV2
gCJD E200K MM
gCJD E200K MV
gCJD E200K VV
% of regions without type II
% of regions with type II
% of regions without type III
% of regions with type III
% of regions without type IV
% of regions with type IV

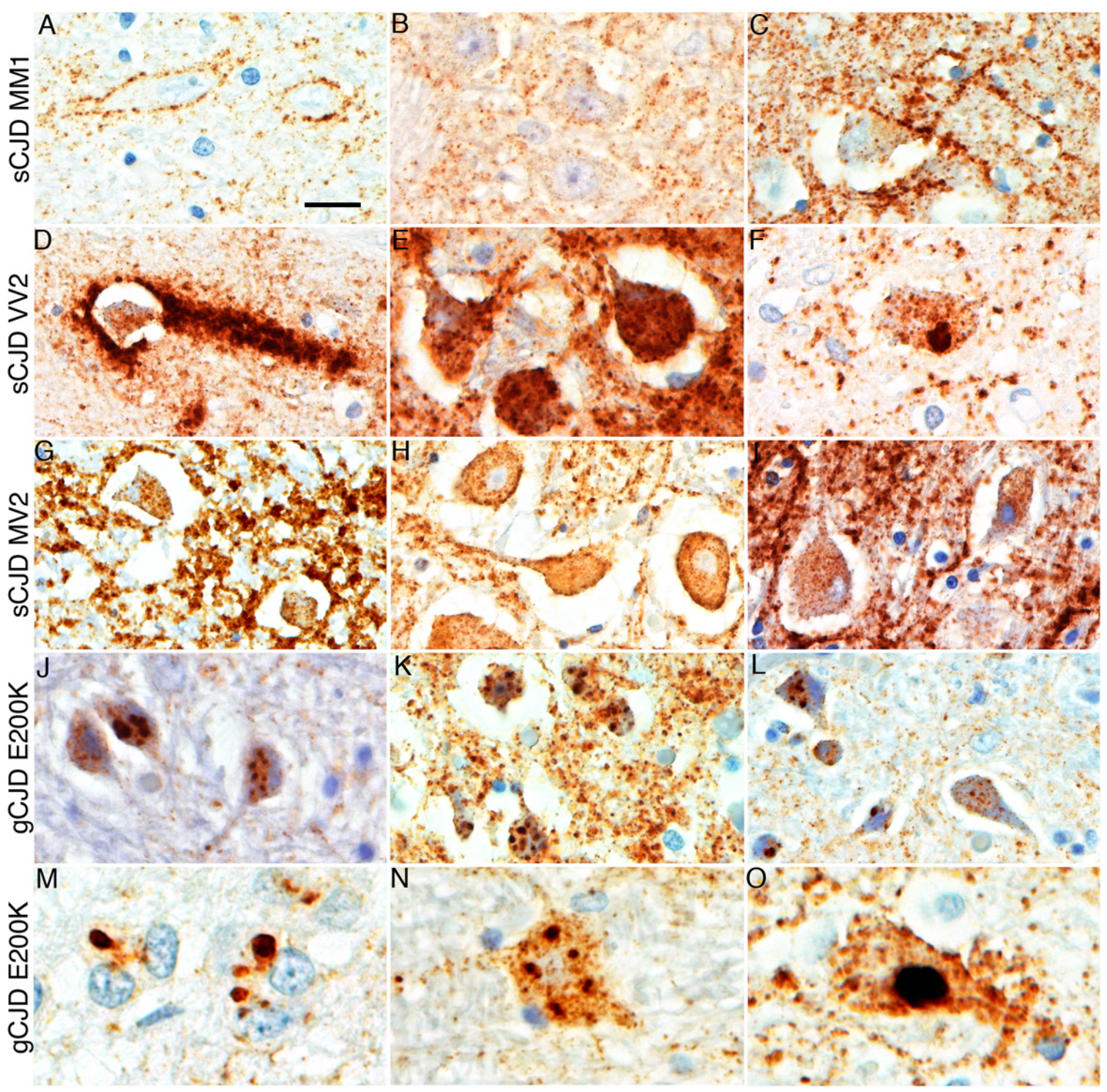
A
B
C
sCJD MM1
D
E
F
sCJD VV2
G
H
I
sCJD MV2
J
K
L
gCJD E200K
M
N
O
gCJD E200K

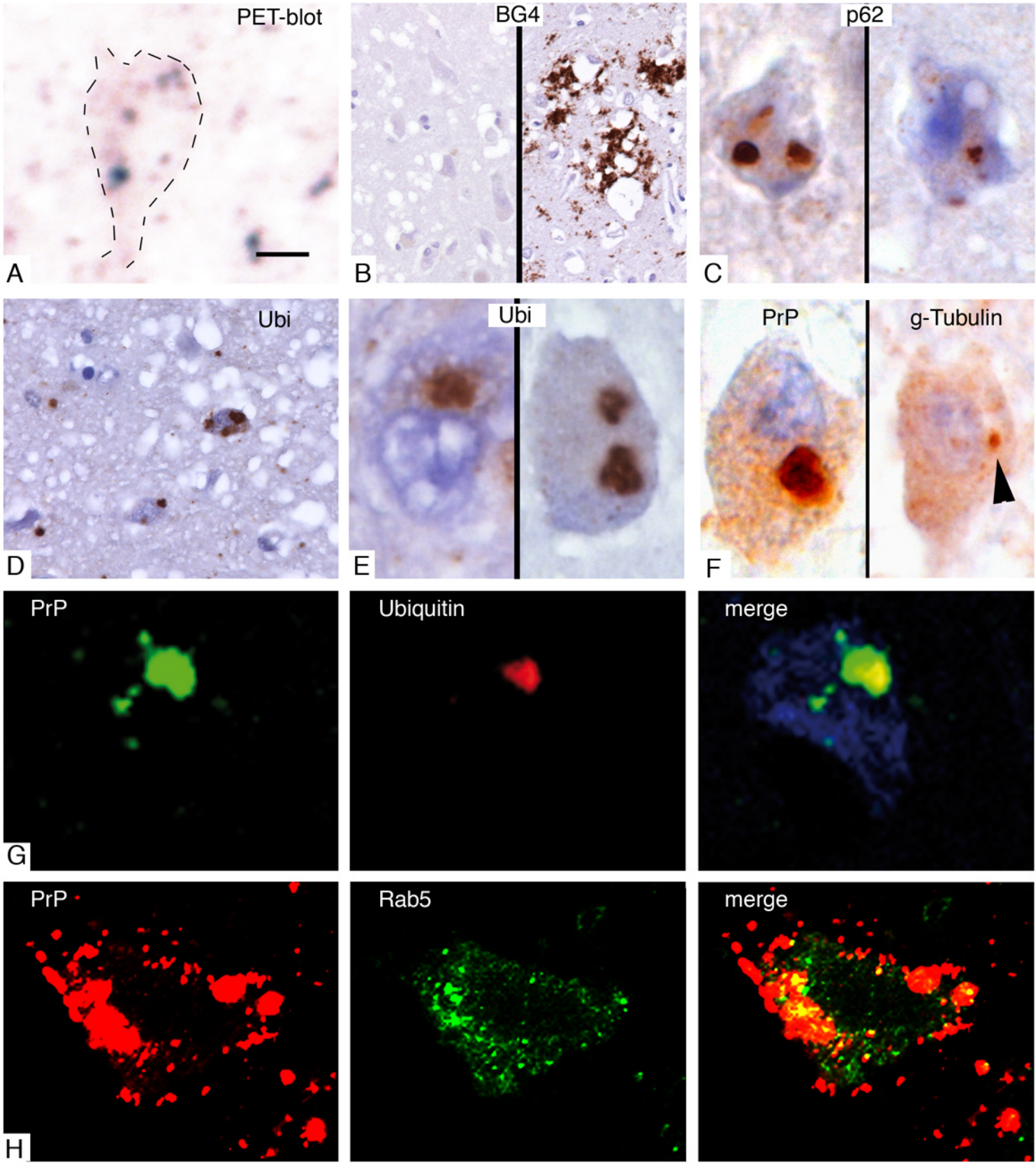
PET-blot
A
BG4
B
p62
C
Ubi
D
Ubi
E
PrP
g-Tubulin
F
PrP
G
Ubiquitin
merge
PrP
H
Rab5
merge

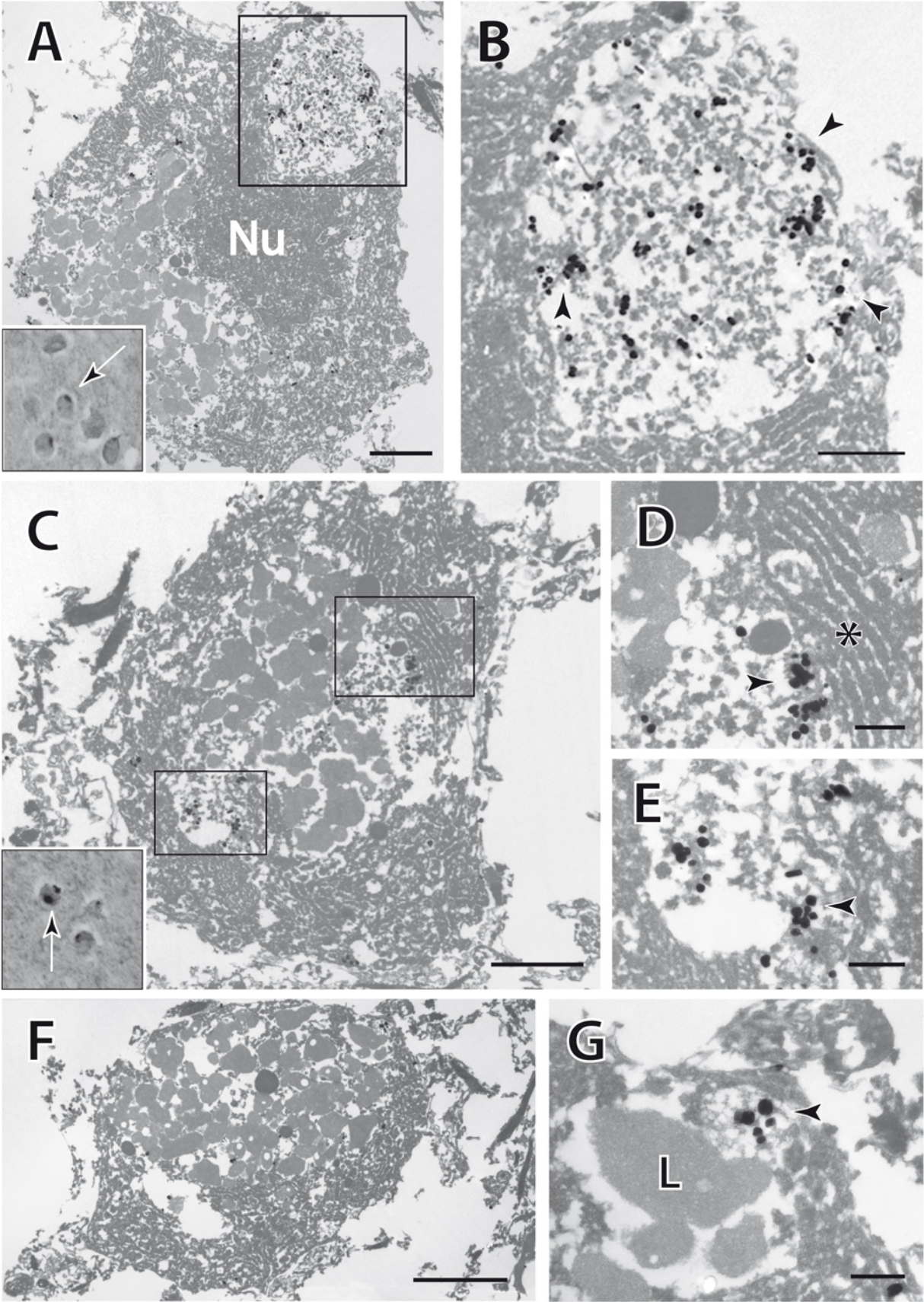
A
Nu
B
C
D
*
E
F
G
L